arXiv:cond-mat/9910325v1 [cond-mat.mes-hall] 21 Oct 1999

TOPOLOGICAL PROPERTIES OF QUANTUM PERIODIC HAMILTONIANS

FRÉDÉRIC FAURE

ABSTRACT. We consider periodic quantum Hamiltonians on the torus phase space (Harper-like Hamiltonians). We calculate the topological Chern index which characterizes each spectral band in the generic case. This calculation is made by a semi-classical approach with use of quasi-modes. As a result, the Chern index is equal to the homotopy of the path of these quasi-modes on phase space as the Floquet parameter θ of the band is varied. It is quite interesting that the Chern indices, defined as topological quantum numbers, can be expressed from simple properties of the classical trajectories.

P.A.C.S. number: 03.65.Sq, 73.50.Jt, 73.40.Hm, 73.20.Dx. key words: semi-classical analysis, tunneling effect, topological numbers, Harper models.

1. INTRODUCTION

Topological quantum numbers are different from quantum numbers based on symmetry because they are insensitive to the imperfections of the systems in which they are observed. In some sense, topological properties are robust properties. Topological quantum numbers have become very important in recent years in condensed matter physics, where measurements of voltage and electrical resistance can be conveniently expressed in terms of them.

If you consider for example a simple model of non-interacting electrons moving in a two-dimensional bi-periodic potential $V(x,y)$ subject to a strong uniform perpendicular magnetic field B_z and a low electrical field E_x, the Hall conductivity σ_{xy} of a given filled Landau electronic band turns out to be proportional to an integer C [1]:

$$\sigma_{xy} = \frac{e^2}{h} C \tag{1}$$

C is the Chern index of the band, describing the topology of its fiber bundle structure [2][3][4][5][6].

We investigate in this paper the value of C as a function of the potential V. In the limit of high magnetic field B_z, the above model is mapped onto the well-known Harper model: the potential V is considered as a perturbation of the cyclotron motion, and the averaging method of mechanics gives an effective Hamiltonian equal to the average of V on the cyclotron circles. We neglect the coupling between the Landau bands [7]. For a high magnetic field, (hence for a small cyclotron radius,) this transformation gives an effective Hamiltonian $H_{eff}(q,p) \sim V(q,p)$, which is bi-periodic in position and momentum (the phase space is a 2D torus), and an effective Planck constant $h_{eff} = hc/(eB)$. In this approximation, trajectories are the contours of $H_{eff} \sim V$. Furthermore, the expression of h_{eff} shows that the high magnetic field regime corresponds to the semi-classical limit. This model will be the starting point of our study in the next section. For the sake of simplicity, we will denote $\hbar_{eff}$ by $\hbar$ in the sequel.

We will restrict ourself to the case where $1/h = N$ is an integer (but this is not a strong restriction as discussed in section 3.1). The spectrum of these Harper-like models has then a finite band structure. To each band $n = 1 \to N$ is associated a topological Chern index C_n. In this paper, we calculate all these Chern indices in the semi-classical limit $N \to \infty$, for a generic Hamiltonian $H(q,p)$ on the torus.

The way we compute these topological indices is the following. First, we use the fact that the classical dynamics generated by H is integrable, to construct quasi-modes (the usual WKB construction) in section 4. An eigen-function $|\varphi_n(\theta_1,\theta_2)>$ of $\hat{H}$ in band n, depends on two quantal parameters related to the periodicity conditions of the wave function on the torus. A quasi-mode $|\tilde{\psi}_n(\theta_1,\theta_2)>$ is a quantum state localized on a trajectory which is very close to $|\varphi_n(\theta_1,\theta_2)>$ in the semi-classical limit $N \to \infty$,[8][9] (except when tunneling effect occurs).

Because of tunneling effect, the eigen-function $|\varphi_n(\theta_1,\theta_2)>$ jumps from one quasi-mode to another one as (θ_1,θ_2) are varying and follows a closed path on the torus. By treating correctly this tunneling effects when it occurs, we obtain a good approximation of the bundle of eigen-functions $|\varphi_n(\theta_1,\theta_2)>$ by quasi modes $|\tilde{\psi}_n(\theta_1,\theta_2)>$, for every value of (θ_1,θ_2). This gives us the principal result of this paper: the Chern index C_n is equal to the homotopy number I_n of this path, on the torus, see eq.(22). We obtain the Chern indices for the whole range of the spectrum, and show that the non-contractible trajectories play a major role.

This result is based on properties presented in the appendix B specific for the computation of the Chern indices. The analytical methods we use rest on properties of zeros of the Bargmann representation (divisors of a holomorphic section). This appendix is self-contained, and general results presented here could be useful for other purposes where topological Chern indices are involved.

There is a constraint on the global spectrum [6][10][5], that $\sum_n C_n = +1$. In section 5, we give an explanation of this in terms of classical trajectories. It is shown that the non-contractible trajectories on the torus are responsible of this fact. This non-trivial total Chern number is crucial for explanation of the Hall conductivity [1]. A natural question is then to determine which bands n have a non zero Chern index C_n in the generic case? We answer this question in section 7, where we explain how to compute the Chern indices of the whole spectrum, from the classical Reeb graph.

Our approach is quite similar to Thouless et al.'s one [1] where they treated $H_\epsilon(q,p) = cos(kq) + \epsilon cos(p)$. The difference is that they treated H_ϵ within a perturbation approximation (with respect to $\epsilon \ll 1$), whereas we use a semi-classical approach. This enables us to treat any generic Hamiltonian H, and to describe new examples with non trivial C_n, different from the Thouless et al.'s one.

Our results extend previous work of the author [11],[12], where the Chern indices were calculated for a restricted range of the spectrum where the classical energy level $\Sigma_E = \{(q,p)/H(q,p) = E\}$ consists in two or three contractible trajectories. In these cases, it was shown that C_n is zero except for special configurations of the trajectories.

We give a numerical illustration of these results in section 6. It is shown that our results, although derived in the semi-classical limit $N \to \infty$, are also valid for quite small N. This illustrates the robustness of the topological properties. This numerical example is also used throughout the paper to confirm our calculations.

In section 8, we complete this work by giving a new (but equivalent) derivation of the interpretation of the Chern index C for conductivity, more intuitive than the usual one based on the Kubo formula [1]: we show here that C is equal to the mean velocity of a wave packet on the torus, when (θ_1,θ_2) move adiabatically.

2. Classical trajectories of a generic Hamiltonian

A generic classical Hamiltonian on the torus is a generic C^∞ Morse function $H(q,p)$ periodic in $q \in I\!R$ and $p \in I\!R$, such that

$$H(q+1,p) = H(q,p+1) = H(q,p). \tag{2}$$

In this section we investigate the topological properties of the trajectories of H, and introduce the Reeb graph [13], which summarizes them. The aim of this paper is to point out the rules that give the Chern indices from the Reeb graph.

A trajectory $q(t), p(t)$ is a solution of the Hamilton equations of motion:

$$\begin{aligned} \partial_t q &= \partial_p H(q,p), \\ \partial_t p &= -\partial_q H(q,p). \end{aligned}$$

The trajectories $q(t), p(t)$ evolve on the plane $I\!R^2$, but because of periodicity, they can be considered as trajectories on the torus T_{qp}, obtained by identifying the opposite sides of the cell $[0,1] \times [0,1]$.

2.1. **Properties on trajectories.** Because of conservation of energy: $d(H(q(t),p(t)))/dt = 0$, each trajectory is included in an energy level $\Sigma_E = \{(q,p)/H(q,p) = E\}$ of the Morse function H. Moreover, the velocity on such a trajectory is never zero, except when there is a critical point of H where $dH = 0$.

We can easily obtain properties on the topology of $\sum_E$:

1. For non critical value of E, Σ_E is a closed one dimensional curve, and each trajectory can be identified with a connected component of Σ_E. Therefore, each trajectory is a periodic orbit, an oriented closed curve on the torus T_{qp}. Its topology (homology) is characterized by two integers $(n_1, n_2)\epsilon Z^2$which are the degrees in the q and p directions of $q(t), p(t)$ for $t = 0 \to T$ where T is the period. (n_1, n_2) are relatively primes, except if $n_1 = 0$ (or $n_2 = 0$) in which case $n_2 = -1, 0$ or $+1$. A contractible trajectory has homology type $n_1 = n_2 = 0$ and is clockwise or anti-clockwise.
2. A generic Hamiltonian has always non contractible closed trajectories with type $(n_1, n_2) \neq (0,0)$. In this case, every other closed trajectory is one of the three types $(n_1, n_2), (-n_1, -n_2)$ or $(0,0)$, and each of these three types exists. (Example: consider a perturbation of $H(q,p) = \cos(n_2 q - n_1 p)$).
3. For non critical value of E, each trajectory belongs locally to a family parameterized by the energy E such that every trajectory has the same type. (The critical trajectories are bifurcations between these families).

For a given generic Hamiltonian, by a good choice of the lattice generators on the plane (q,p), it is possible to deal with trajectories of types $(0,0)$ $(0,+1)$ and $(0,-1)$ only. We will adopt this choice in the sequel of this paper.

Now concerning the critical points and the critical trajectories :

1. There are three sorts of critical points: a local minimum, a saddle point or a local maximum. From Euler formula ([14] p.29) we have $\#(mins) + \#(maxs) - \#(saddles) = 0$ (The Euler characteristic of the torus is 0).

2.2. **Example.** We will give now an example in order to illustrate these statements. This example will be used throughout the paper.

Consider the following Hamiltonian:

$$\begin{aligned} H(q,p) &= H_0(q,p) + H_1(q,p), \\ H_0(q,p) &= \cos(2\pi q) + 0.1\cos(2\pi p), \\ H_1(q,p) &= P\left[\exp\left(-100(q-q_0)^2 - 10(p-p_0)^2\right)\right], \end{aligned} \tag{3}$$

where P is a functional operator which sums the function in each cell and makes it periodic:

$$P\left[f(q,p)\right]=\sum_{i,j}f(q+i,p+j).$$

The trajectories generated by H are shown on the figure 1, for $q_0=0.45$, $p_0=0.45$. There are one minimum F, two maxima A,D, and three saddle points B,C,E.

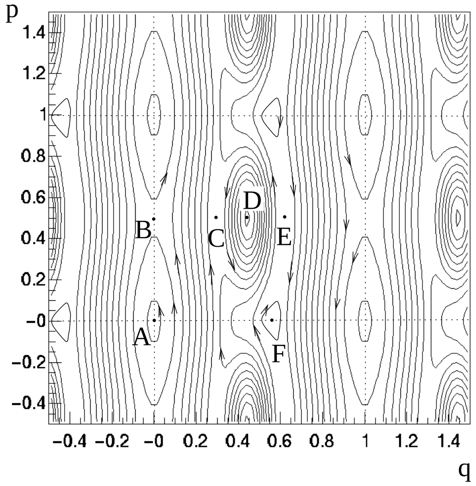

FIGURE 1. Trajectories and fixed points of Hamiltonian (3).

The figure 2 gives a schematic view of the families of trajectories, with their bifurcations, and homology types. It is called a "Reeb graph" $\mathcal{R}$ [13]. By definition, it is the topological quotient space $\mathcal{R}=T_{qp}/\mathcal{F}$ where $\mathcal{F}=\{\Sigma_E\}_E$ is the set of energy levels. The topology of this graph gives the relative location of the trajectories (the q variable here is only to indicate that the dashed line can be obtained by a section at constant p in figure 1).

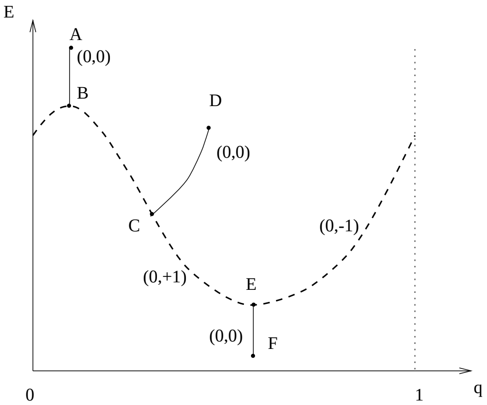

FIGURE 2. Reeb graph of H: a schematic view of the Trajectories types and bifurcations of Hamiltonian (3). Each point of the dashed line corresponds to a non contractible trajectory. They form a one-dimensional family. Each point of a solid line corresponds to a contractible trajectory.

The Reeb graph can be done for any given generic Hamiltonian. This figure will always have a similar apparency, with one transverse (dashed) line (from $q=0$

to $q = 1$) corresponding to the non contractible trajectories, and branches from it (solid lines), corresponding to contractible trajectories. Critical energies are at the extremities of these branches. The final value of the Chern indices will be read more or less directly from this graph in section 7.

3. The Quantum Hamiltonian

In this section we introduce well known material that will be useful for the sequel.

3.1. **The Hilbert space $\mathcal{H}_P$ of the plane .** The Hilbert space corresponding to the classical motion in the plane phase space $T^*(I\!\!R) \cong I\!\!R^2$ is

$$\mathcal{H}_P = L^2(I\!\!R),$$

(the index P will remind us that we deal with the plane phase-space).

We choose a symmetric quantization procedure: to the classical Hamiltonian $H(q,p)$ we associate a self-adjoint operator $\hat{H}$ in $\mathcal{H}_P$ by

$$\hat{H} = \sum_{n_1,n_2 \in Z^2} \frac{1}{2} c_{n_1,n_2} \exp(i2\pi n_1 \hat{q}) \exp(i2\pi n_2 \hat{p}) + \text{hermitian conjugate.}$$

Where $c_{n_1 n_2}$ are the Fourier components of the function $H(q,p)$:

$$H(q,p) = \sum_{n_1,n_2 \in Z^2} c_{n_1,n_2} \exp(i2\pi n_1 q) \exp(i2\pi n_2 p). \tag{4}$$

Since H is a real valued function, the complex coefficients $c_{n_1 n_2}$ must satisfy:

$$c_{n_1,n_2} = \bar{c}_{-n_1,-n_2} \in \mathbb{C}, \quad (n_1,n_2) \in \mathbb{Z}^2.$$

We denote by $\hat{T}_Q$[respectively $\hat{T}_P$] the translation operator by one period: $\hat{T}_Q$ translates by $Q = 1$ a wave function $\psi(x)$ and $\hat{T}_P$ translates its Fourier transform $\hat{\psi}(p)$ by $P = 1$:

$$\hat{T}_Q \psi(x) = \psi(x-1) \tag{5}$$

$$\hat{T}_P \hat{\psi}(p) = \hat{\psi}(p-1). \tag{6}$$

We may rewrite equations (5) and (6) as:

$$\hat{T}_Q = \exp(-i\hat{p}/\hbar), \quad \hat{T}_P = \exp(i\hat{q}/\hbar).$$

Quantum mechanically speaking, the periodicity Eq. (2) reads:

$$[\hat{H}, \hat{T}_Q] = [\hat{H}, \hat{T}_P] = 0. \tag{7}$$

To continue, we now have to assume that

$$[\hat{T}_Q, \hat{T}_P] = 0. \tag{8}$$

It is easy to prove that:

$$\hat{T}_Q \hat{T}_P = e^{-i/\hbar} \hat{T}_P \hat{T}_Q,$$

hence (8) is fulfilled if and only if there exists an integer N such that:

$$N = \frac{1}{h} \in I\!\!N^*. \tag{9}$$

with $h = 2\pi\hbar$. This hypothesis (9) can be regarded as a geometric quantization condition, which states that there is an integer number of Planck cells in the phase space. The semi-classical limit $\hbar \to 0$ corresponds then to the limit $N \to +\infty$.

We now assume that hypothesis (9) is fulfilled.

Note that hypothesis is not so restrictive, because any value of h can be well approximated by a rational number $h = m/N$. It is then easy to check that $[\hat{T}_{mQ}, \hat{T}_P] = 0$. In this case we just have then to consider the torus phase space $[0, mQ[\times]0, P[$ instead of $[0, Q[\times]0, P[$.

3.2. **The Hilbert space $\mathcal{H}_T(\theta_1,\theta_2)$ for the torus.** According to the commutation relations (7) and (8), the Hilbert space $L^2(\mathbb{R})$ may be decomposed as a direct sum of the eigen-spaces of the translation operators $\hat{T}_Q$ and $\hat{T}_P$:

$$\begin{aligned} \mathcal{H}_P = L^2(\mathbb{R}) &= \int\int \mathcal{H}_T(\theta_1,\theta_2)\,\frac{d\theta_1 d\theta_2}{(2\pi)^2} \\ \mathcal{H}_T(\theta_1,\theta_2) &= \left\{ |\psi> \text{ such that } \left\{ \begin{array}{l} \hat{T}_Q|\psi>=\exp(i\theta_1)|\psi> \\ \hat{T}_P|\psi>=\exp(i\theta_2)|\psi> \end{array} \right\} \right\}, \end{aligned} \tag{10}$$

with $(\theta_1,\theta_2) \in [0,2\pi[^2$ related to the periodicity of the wave function under translations by an elementary cell. The space of the parameters (θ_1,θ_2) has also the topology of a torus, and will be denoted by T_θ.

The space $\mathcal{H}_T(\theta_1,\theta_2)$ is not a subspace of $L^2(\mathbb{R})$, the space of physical states, it is a space of distributions in the x representation.

It is well known that $H_T(\theta_1,\theta_2)$ is finite dimensional [1]. To see that, let $|\psi>\in \mathcal{H}_T(\theta_1,\theta_2)$. The Fourier transform of $\psi(x)$ is θ_2-Floquet-periodic of period P, so $\psi(x)$ is discrete, it is a sum of Dirac distributions supported at points distant from $h=1/N$ from each other. Moreover, $\psi(x)$ is θ_1-periodic, hence ψ is characterized by the N coefficients at the N Dirac distributions supporting points in the interval $q\in[0,1[$.

Explicitly, a basis of $\mathcal{H}_T(\vec{\theta})$ is given by N distribution denoted $|j,\vec{\theta}>$:

$$|j,\vec{\theta}> \equiv \psi_{j,\vec{\theta}}(x) = \frac{1}{\sqrt{N}}\sum_{n_1\in\mathbb{Z}} \exp\left(-in_1\theta_1\right)\delta(x-q_j-n_1), \quad j=1,\dots,N$$

$$\text{with } q_j = \frac{1}{N}\left(j+\frac{\theta_2}{2\pi}\right).$$

Eventually we get:

$$\dim_{\mathbb{C}}\ \mathcal{H}_T(\theta_1,\theta_2) = N.$$

Because of Eq.(7) the Hamiltonian $\hat{H}$ is block-diagonal with respect to the decomposition Eq.(10). The operator $\hat{H}$ acts on $\mathcal{H}_T(\theta_1,\theta_2)$ as a $N\times N$ hermitian matrix, its spectrum $\sigma(\theta_1,\theta_2)$ is made of N eigenvalues and N corresponding eigenfunctions:

$$\hat{H}|\varphi_n(\theta_1,\theta_2)>=E_n(\theta_1,\theta_2)|\varphi_n(\theta_1,\theta_2)>, \quad n=1,\dots,N. \tag{11}$$

For a given level n, assuming that $E_n(\theta_1,\theta_2)$ is never degenerate $\forall\theta$, the energy level $E_n(\theta_1,\theta_2)$ forms a band as $(\theta_1,\theta_2)\in T_\theta$ are varying, and the eigenvectors $|\psi_n(\theta_1,\theta_2)>$ form a $2D$ surface in the quantum states space. But for a fixed (θ_1,θ_2), and any $\lambda\in\mathbb{C}$, $\lambda|\psi_n(\theta_1,\theta_2)>$ is also an eigenvector. So for a fixed level n, the family of eigenvectors form a complex-line-bundle (of fiber $\cong \mathbb{C}\ni\lambda$) in the projective space of the bundle $\mathcal{H}_T\to T_\theta$. The topology of this line bundle is characterized by an integer $C_n\in\mathbb{Z}$, called the Chern index ([15], chap 1, p.139).

The definition of this topological Chern index is presented in section 5.1.

3.3. **The Hilbert space $\mathcal{H}_C(\theta_2)$ for the cylinder.** In the sequel it will be useful to consider an intermediate decomposition of $\mathcal{H}_P$ in terms of states periodic in momentum only:

$$\mathcal{H}_P = L^2(\mathbb{R}) = \int \mathcal{H}_C(\theta_2)\frac{d\theta_2}{2\pi}$$

$$\mathcal{H}_C(\theta_2) = \left\{|\psi> \text{ such that } \hat{T}_P|\psi>=\exp(i\theta_2)|\psi>\right\}.$$

Each state in $\mathcal{H}_C(\theta_2)$ is a sum of Dirac distributions supported at points $q_n = \frac{1}{N}\left(n+\frac{\theta_2}{2\pi}\right)$ with $n\in\mathbb{Z}$. The weights belongs to $l^2(\mathbb{Z})$.

Conversely:

$$\mathcal{H}_C(\theta_2) = \int \mathcal{H}_T(\theta_1, \theta_2) d\theta_1.$$

For each θ_2, the Hilbert space $\mathcal{H}_C(\theta_2)$is associated with the cylinder phase space denoted C_{qp}, where $(q,p) \in I\!R^2$ is identified with $(q, p+1)$.

From a state $|\psi_P> \in \mathcal{H}_P = L^2(I\!R)$ of the plane, we can construct a state $|\psi_C> \in \mathcal{H}_C(\theta_2)$ of the cylinder by the operation:

$$|\psi_C(\theta_2)>= P_{\theta_2}|\psi_P>= \sum_{n=-\infty}^{+\infty} \exp(-in\theta_2) T_P^n |\psi_P> . \tag{12}$$

From a state $|\psi_C> \in \mathcal{H}_C(\theta_2)$ of the cylinder, we can construct a state $|\psi_T(\theta_1,\theta_2)> \in \mathcal{H}_T(\theta_1,\theta_2)$ of the torus by the operation:

$$|\psi_T(\theta_1,\theta_2)>= P_{\theta_1}|\psi_C(\theta_2)>= \sum_{n=-\infty}^{+\infty} \exp(-in\theta_1) T_Q^n |\psi_C(\theta_2)> . \tag{13}$$

4. THE QUASI MODES

4.1. Construction of a quasi-mode.

The W.K.B. method allows the construction of a quasi-modes for integrable dynamics. See [8], Lazutkin [9] p. 235.

First, we recall the definition and general properties of quasi-modes.

Definition 1. If Γ is a given closed trajectory with energy E, a quasi-mode with error ϵ, is a quantum state $|\tilde{\psi}>$ localized near Γ, which satisfies:

$$\left\| \hat{H}|\tilde{\psi}> - \tilde{E}|\tilde{\psi}> \right\| = \epsilon = o(h^\infty),$$

with $h = 1/N$ going to zero, with $(E - \tilde{E}) = o(h)$. The trajectory Γ is called the support of $|\tilde{\psi}>$ and noted

$$\Gamma = \text{Supp}(|\tilde{\psi}>).$$

If we want to improve this error ϵ (and have an error exponentially small with respect to h), we have to take into account tunneling effect between Γ, and Γ' the "closest" trajectory Γ' which has the same energy E. ([16],[17],[18]). We will come back on this point.

Proposition 1. [9]

The interval $[\tilde{E} - \epsilon, \tilde{E} + \epsilon]$ *contains at least one eigenvalue of* $\hat{H}$.

Let $\Delta_\alpha = [\tilde{E} - \alpha, \tilde{E} + \alpha]$. *If* Δ_α *contains only one eigen-value* E^*, *with eigenvector* $|\varphi>$, *then (for normalized vectors)*

$$\exists \beta \in R, \qquad \left\| |\varphi> - e^{i\beta}|\tilde{\psi}> \right\| \leq \frac{\epsilon}{\alpha}, \tag{14}$$

consequently, $<\varphi|\tilde{\psi}> \neq 0$ *as soon as* $\epsilon \leq \alpha\sqrt{2}$ *(for our purpose, we will say in that case, that* $|\tilde{\psi}>$ *is a "good approximation" of* $|\varphi>$. *This condition will be sufficient to construct a bundle of quasi-modes with the same topology, same Chern index).*

Let us now give properties of quasi-modes specific to our problem. The explicit construction of the quasi-modes can be found in [19][20][21].

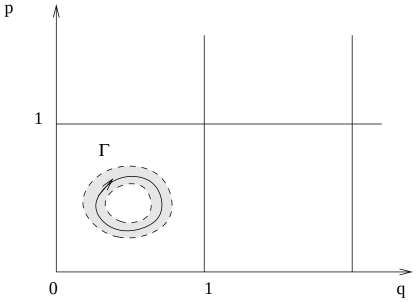

FIGURE 3. Quasi-mode localized on a trajectory Γ of type $(0,0)$ in cell $(0,0)$.

Contractible trajectories of type $(0,0)$. For a non critical contractible trajectory Γ of type $(0,0)$, we first construct a quasi-mode on the plane, $|\tilde{\psi}_P> \in \mathcal{H}_P$. From the usual W.K.B construction, this quasi mode is localized on a single image of Γ, for example in the cell $(0,0)$. See figure 3.

The energy $\tilde{E}$ of this quasi-mode is given by the usual E.B.K. condition:

$$S(\tilde{E}) = (k+1/2)h + o(h) \quad , \quad k \in \mathbb{Z},$$

with $S(\tilde{E})$ the surface inclosed in the trajectory Γ.

A quasi-mode $|\tilde{\psi}_C(\theta_2)>$ on the cylinder can be deduced by eq.(12). A quasi-mode $|\tilde{\psi}_T(\theta_1,\theta_2)>$ on the torus can be constructed by eq.(13). Note that the energy of these quasi-modes $\tilde{E}$ doesn't depend on (θ_1,θ_2).

Non contractible trajectories of type $(0,\pm 1)$. If Γ is a non critical trajectory with type $\vec{n} = (0,\pm 1)$, Γ is closed on the cylinder C_{qp} and a quasi-mode $|\tilde{\psi}_C(\theta_2)> \in \mathcal{H}_C(\theta_2)$ can be constructed for every θ_2.

$|\tilde{\psi}_C(\theta_2)>$ is localized on Γ, for example in cell 0, see figure 4.

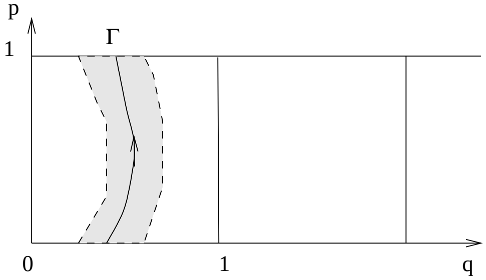

FIGURE 4. Quasi-mode localized on a trajectory Γ of type $(0,+1)$, in cell (0) on the cylinder.

The energy $\tilde{E}$ of this quasi-mode is given by the condition:

$$S(\tilde{E}) = (k - \theta_2/2\pi)h + o(h), \quad k \in \mathbb{Z}, \tag{15}$$

where $S(\tilde{E})$ is the surface included in the unit cell, on the right of the trajectory Γ (here oriented by increasing p). We justify this condition in the next paragraph.

Note that the energy $\tilde{E}(\theta_2)$ as well as the support $\Gamma(\theta_2)$ depend continuously on θ_2.

A quasi mode $|\tilde{\psi}_T(\theta_1,\theta_2)>$ on the torus can be deduced from $|\tilde{\psi}_C(\theta_2)>$by eq.(13).

For contractible and non contractible trajectories, an other quasi-mode with the same energy can be constructed in the cell n by

$$|\tilde{\psi}_{C,n}(\theta_2)>=T_Q^n|\tilde{\psi}_C(\theta_2)> . \tag{16}$$

From the W.K.B. construction, the error ϵ of these quasi-modes is of order $o(h^\infty)$. The error ϵ is due to tunneling interaction with "the nearest quasi-mode of nearby energy" (see the next section).

Critical trajectories. If E_0 is a critical energy, quasi modes of energy near E_0 (in the interval $[E_0 \pm O(h)]$) and localized near the critical trajectory, can be constructed. See [22][23][24].

Justification of quantization rule eq.15. When constructing a WKB quasi-mode on a closed trajectory, the quantization rule comes from the phase matching. The phase of the Fourier transform of the quasi-mode evolves like $(-\int qdp)$ along the trajectory $q(t), p(t)$. For a trajectory Γ of type $(0, \pm1)$, the phase accumulated over a period is then $\varphi = S/\hbar = -\int_\Gamma qdp/\hbar$, where S is the surface on the right of the trajectory Γ (oriented by increasing value of p). The periodicity condition (10) requires that $\varphi = \theta_2 \quad [2\pi]$. This gives the result (15).

4.2. **The semi-classical spectrum without tunneling corrections.** We now investigate the global properties of the quasi-modes, with respect to θ_2.

Consider fixed values of $(\theta_1, \theta_2) \in T_\theta$. A W.K.B. construction as previously described, gives us N quasi-modes $|\tilde{\psi}_T(\theta_1, \theta_2)>_n$ with energies $\tilde{E}_n(\theta_1, \theta_2)$ over the whole energy range, with $n = 1 \rightarrow N$. This is a semi-classical approximation $\sigma_{sc}(\theta_1, \theta_2)$ of the spectrum $\sigma(\theta_1, \theta_2)$ defined by eq.(11). In fact the construction was made on $\mathcal{H}_C(\theta_2)$ and does not depend on θ_1, so we will note it $\sigma_{sc}(\theta_2)$. (For contractible trajectories, it does not even depend on θ_2).

From the above construction, each quasi-mode $|\tilde{\psi}_C(\theta_2)>$ depends continuously on θ_2. So each quasi-mode belongs to a function $\Psi : \theta_2 \rightarrow |\tilde{\psi}_C(\theta_2)> \in \mathcal{H}_C(\theta_2)$ which is periodic with respect to θ_2 (up to a phase), with a period $\Theta_2 = 2\pi m$, with $m \in N$. (Otherwise, if the function Ψ were not periodic, the spectrum $\sigma_{sc}(\theta_2)$ would be infinite for a fixed value of θ_2). The corresponding energy $\tilde{E}(\theta_2)$ and the support $\Gamma(\theta_2)$ are therefore also periodic with the same periods.

If the trajectory Γ is contractible (type $(0,0)$), the energy $\tilde{E}$ and the support Γ are fixed. They do not depend on θ_2, and the period is $\Theta_2 = 2\pi$.

For a non contractible and non critical trajectory (type $(0, \pm1)$), eq.(15) tells that the surface $\theta_2 \rightarrow S(\theta_2)$ on the right of Γ is a strictly decreasing function because $dS/d\theta_2 = -h/2\pi$. Then $\theta_2 \rightarrow \Gamma(\theta_2)$ moves from the left to the right on the set of non contractible trajectories on the cylinder C_{qp}. This function reaches all the non contractible trajectories, and jumps over a connected component of contractible trajectories, via a critical point . See figure 5.

The surface $S(\theta_2)$ is always a decreasing function, but the corresponding energy $E(\theta_2)$ decreases for trajectories of type $(0, +1)$ and increases for type $(0, -1)$, with the behavior shown on figure 2, if we plot $E(\theta_2)$ for $\theta_2 = 0 \rightarrow 2\pi m$. Figure 6 shows this function $E(\theta_2)$ but folded in the interval $\theta_2 = 0 \rightarrow 2\pi$.

So we obtain:

Proposition 2.

The global spectrum $\theta_2 \rightarrow \sigma_{sc}(\theta_2)$ is the union of ***one single*** *function $\Psi_{nc} : \theta_2 \rightarrow |\tilde{\psi}_{nc}(\theta_2)> \in \mathcal{H}_C(\theta_2)$, and many others $(\Psi_c)_{i=1,..,N_c} : \theta_2 \rightarrow |\tilde{\psi}_c(\theta_2)> \in \mathcal{H}_C(\theta_2)$ such that*

The support Γ_{nc} of Ψ_{nc} is on the non contractible trajectories. The period of Ψ_{nc} is $\Theta_2 = 2\pi.N_{nc}$, such that $N_{nc}.h \sim S_{nc}$ the surface occupied by the non-contractible

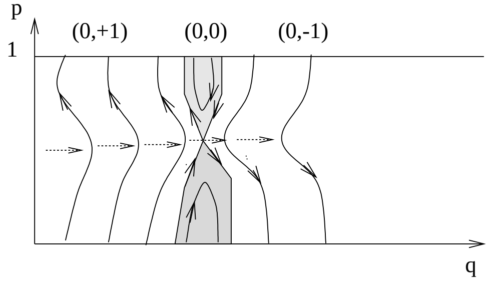

FIGURE 5. The dashed arrows indicate the motion of the support of a quasi mode, $\theta_2 \to \Gamma(\theta_2)$, over all non contractible trajectories, as θ_2 increases.

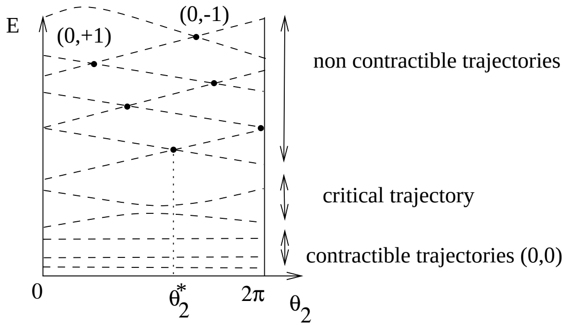

FIGURE 6. The energy of the quasi-modes as a function of θ_2.

trajectories. In phase space, this support $\theta_2 \to \Gamma_{nc}(\theta_2)$ *is a closed cycle of homotopy 1 on the cylinder* C_{qp}*.*

The support Γ_c *of each function* $(\Psi_c)_i$ *is on a fixed contractible trajectory. Its period is* $\Theta_2 = 2\pi$*. The number* N_c *of these functions is such that* $N_c.h \sim S_c$ *the surface occupied by the contractible trajectories. Note that* $N = N_c + N_{nc}$ *and* $1 = S_{nc} + S_c$*.*

We now discuss the error of the spectrum $\sigma_{sc}(\theta_2)$.

The error of each quasi-mode is $\epsilon \sim o(h^\infty)$. There are crossings in the spectrum $\sigma_{sc}(\theta_2)$ for discrete values θ_2^*, (caused by the non contractible function when $\tilde{E}_{nc}(\theta_2) = \tilde{E}_{nc}(\theta_2^{'})$ or $\tilde{E}_{nc}(\theta_2) = \tilde{E}_c(\theta_2^{'})$), see figure 6. For fixed θ_2, away from a small neighborhood of every crossing value θ_2^*, the spectrum $\sigma_{sc}(\theta_2)$ has N discrete eigenvalues and each eigen-value is isolated from the overs by an interval of length $\alpha \gg \epsilon$. We deduce from properties 1 that the corresponding quasi-modes $|\tilde{\psi}_n(\theta_2) >$ (in fact their image in $\mathcal{H}_T$ by the mapping P_{θ_2}), are a good approximation of the actual eigenvectors $|\varphi_n(\theta_1, \theta_2) >$, for any θ_1.

Let us remark that this semi-classical spectrum $\sigma_{sc}(\theta_2)$ does not depend on θ_1 and is thus infinitely degenerate. This correspond to the invariance by the translation (16). This is not the case in the actual spectrum $\sigma(\theta_1, \theta_2)$ because of tunneling effect.

Figure 9 shows the numerical spectrum of our example $H(q, p)$, eq.(3). From this, we deduce what the semi-classical spectrum should look like: fig (10). Compare this with the semi-classical spectrum figure 6.

$\sigma_{sc}(\theta_2)$ is not a good approximation of the actual spectrum near the crossing values θ_2^*. To improve that, in the next section, we will take into account the tunneling effect at each crossing of energy. It causes a splitting of levels and we will recover N well defined bands of energy.

4.3. **The semi-classical spectrum with tunneling corrections.** Consider a neighborhood U of a value θ_2^*, where there is a crossing in the spectrum $\sigma_{sc}(\theta_2)$ between two energies: $\tilde{E}_1(\theta_2^*) = \tilde{E}_2(\theta_2^*)$. See figure 6. As said before, this crossing is caused two non contractible trajectories when $\tilde{E}_{nc}(\theta_2) = \tilde{E}_{nc}(\theta_2^{'})$ or by one non contractible trajectory and one contractible one: $\tilde{E}_{nc}(\theta_2) = \tilde{E}_c$. The crossing due to two contractible trajectories $\tilde{E}_{c1} = \tilde{E}_{c2}$ is not considered here, because it does not occur for a generic Hamiltonian H. See [11][12] for results treating this non generic case. From eq.(16), these energies correspond to two families of quasi-modes: $|\tilde{\psi}1_{C,n_1}>$, $|\tilde{\psi}2_{C,n_2}>\in \mathcal{H}_C(\theta_2)$ where $n_1 \in \mathbb{Z}$, $n_2 \in \mathbb{Z}$. We suppose that these quasi-modes are localized respectively on two trajectories Γ_1 and Γ_2, in cells n_1 and n_2.

To improve the error ϵ of the quasi-mode say $|\tilde{\psi}1_{C,n_1}>$, we have to take into account the tunneling interactions with other quasi-modes which have nearby energy $|\tilde{\psi}j_{C,m}>$with $j = 1, 2$ and $m \in \mathbb{Z}$. See figure 7. This tunneling interaction comes from non vanishing terms $A_{j,m} =<\tilde{\psi}1_{C,n_1}|\hat{H}|\tilde{\psi}j_{C,m}>$. We will treat the tunneling effect at the leading order, by keeping only the dominant term. Consider first the terms A_{2,n_2} with $j = 2$, and $n_2 \in \mathbb{Z}$. We keep the n_2 term with greatest modulus: $|A_{2,n_2}|$. This term is $o(h^\infty)$ and describe the tunneling interaction between $|\tilde{\psi}1_{C,n_1}>$and the "nearest" quasi-mode $|\tilde{\psi}2_{C,n_2}>$. See figure 7. It is clear that the nearest quasi-mode is $n_2 = n_1$ or $n_2 = n_1 \pm 1$, because other values of n_2 are in more distant cells. The other terms are $o(h^\infty)$ with respect to leading order term. Consider now the terms $A_{1,m}$ with $j = 1$, and $m \in \mathbb{Z}$. The dominant term is for $m = n_1$: $A_{1,n_1} =<\tilde{\psi}1_{C,n_1}|\hat{H}|\tilde{\psi}1_{C,n_1}>= \tilde{E}_1(\theta_2)$. This is the energy of the quasi-mode. The others terms, which describe tunneling interaction between $|\tilde{\psi}1_{C,n_1}>$ and its images $|\tilde{\psi}1_{C,m}>$ in other cells, are $o(h^\infty)$ with respect to $|A_{2,n_2}|$ and so negligible.

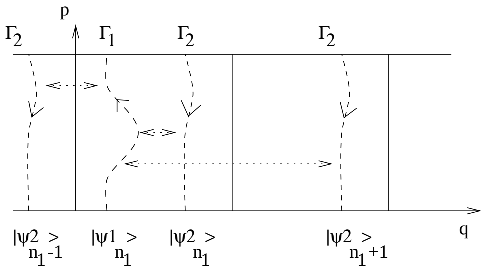

FIGURE 7. Tunneling effect between quasi-mode $|\psi1_{n1}>$ on trajectory Γ_1, in cell n_1, and quasi-modes $|\psi2_{n2}>$. We keep only the dominant tunneling interaction, here due to $|\psi2_{n1}>$.

We have obtained that the dominant correction to the quasi-modes $|\tilde{\psi}1_{C,n_1}>$ is described by the 2×2 tunneling interaction matrix:

$$A(\theta_2) = \left(<\tilde{\psi}i_{C,n_1}|\hat{H}|\tilde{\psi}j_{C,n_2}>\right)_{i,j} = \begin{pmatrix} \tilde{E}_1(\theta_2) & A_{2,n_2}(\theta_2) \\ \overline{A_{2,n_2}}(\theta_2) & \tilde{E}_2(\theta_2) \end{pmatrix},$$

where $|\tilde{\psi}2_{C,n_2}>$ is the "nearest" quasi-mode to $|\tilde{\psi}1_{C,n_1}>$, $n_2 = n_1$ or $n_2 = n_1 \pm 1$, and $|A_{2,n_2}|$ is $o(h^\infty)$.

By diagonalizing the matrix A, we obtain two quasi-modes $|\tilde{\psi}_{C+}(\theta_2)>$ and $|\tilde{\psi}_{C-}(\theta_2)>\in \mathcal{H}_C(\theta_2)$ expressed as a linear superposition of $|\tilde{\psi}1_{C,n_1}>$and $|\tilde{\psi}2_{C,n_2}>$, and two energies $E_+(\theta_2) > E_-(\theta_2)$ with a gap $|\tilde{E}_+(\theta_2) - \tilde{E}_-(\theta_2)| \geq |A_{2,n_2}|$. But the error of the quasi-modes is $o(h^\infty)$ with respect to this gap. From property (1), we deduce that these quasi-modes $|\tilde{\psi}_{C\pm}(\theta_2)>$ (their image in $\mathcal{H}_T$ actually) are a good approximation of the eigenvectors $|\varphi_i(\theta_1, \theta_2)>$, for any θ_1.

Now if we match these results with the outside of the neighborhood U of θ_2^*, we can obtain a continuous dependence of $|\tilde{\psi}_C(\theta_2)>$with respect to $\theta_2 \in I\!R$.

Proposition 3. *We have obtained quasi-modes* $|\tilde{\psi}_C(\theta_2)>$ *on the cylinder, which are a good approximation of the spectrum eq.(11) for any* θ_1, θ_2 *in the sense that :*

$$< \varphi_n(\theta_1, \theta_2) | \tilde{\psi}_T(\theta_1, \theta_2) > \neq 0 \text{ for every } (\theta_1, \theta_2). \tag{17}$$

We note this approximate spectrum by $\sigma_{sc,t}(\theta_2)$ *(the energies do not depend on* θ_1*).*

There is no more crossing in the energy levels, so we have N *well defined (semi-classical) bands and corresponding quasi-modes* $|\tilde{\psi}_{C,n}(\theta_2)>$, $n = 1, .., N$.

At each avoided crossing, we have obtained that the support of a quasi-mode jumps from the trajectory Γ_1 *in cell* n_1 *(resp.* Γ_2 *in* n_2*) to the closest trajectory* Γ_2 *in cell* $n_2 = n_1$ *or* $n_2 = n_1 \pm 1$ *(respect.* Γ_1 *in* n_1 *) as in figure 7.*

More globally, for each band n*, we derived an function for the support of the quasi-mode* $|\tilde{\psi}_{C,n}(\theta_2)>$*on the cylinder* C_{qp}*:*

$$S_{Cn}: \quad \theta_2 \in R \to Supp\left(|\psi_{C,n}(\theta_2)>\right) \quad \subset C_{qp}. \tag{18}$$

The image $S_{T,n}$ *of* $S_{C,n}$ *on the torus is periodic for* $\theta_2 = 0 \to 2\pi$*, and* $S_{C,n}$ *is a lifting of* $S_{T,n}$ *on the cylinder. With* $S_{C,n}$ *is associated a homotopic number* $I_n \in Z\!\!Z$*. Precisely,* I_n *is given by:*

$$T_Q^{I_n}\left[Supp\left(|\psi_{C,n}(0)>\right)\right] = \left[Supp\left(|\psi_{C,n}(2\pi)>\right)\right]. \tag{19}$$

I_n *is simply the result of the jumps of the quasi-mode from cell* n_1 *to cell* $n_1 + I_n$ *as* $\theta_2 = 0 \to 2\pi$*.*

5. Chern indices

5.1. **Definition .** The eigen-functions $|\varphi_n(\theta_1, \theta_2)>$ of the band n, eq.(11), form a complex line fiber bundle over the torus $(\theta_1, \theta_2) \in T_\theta$. On a contractible subset of $U \subset T_\theta$ we can choose the states $|\varphi_n(\theta_1, \theta_2)>$ such that they are normalized and that they form a (continuous) section over U. Note that this is not possible over the whole torus T_θ except if the bundle is trivial.

The global topology of this complex line bundle is characterized by its Chern index ([15] p. 139, [25]).

Because of the natural Hilbert scalar product on $L^2(I\!R) = \int\int \mathcal{H}_T(\theta_1, \theta_2)\, d\theta_1 d\theta_2$, which induces the Berry (or Chern) connection ([26], [2]), this topological number is explicitly given by the integral of the Berry (or Chern) curvature ([1],[15] p. 141):

$$C_n = \frac{i}{2\pi} \int_{T_\theta} \left(< \partial_{\theta_1}\varphi_n | \partial_{\theta_2}\varphi_n > - < \partial_{\theta_2}\varphi_n | \partial_{\theta_1}\varphi_n >\right) d\theta_1 d\theta_2, \tag{20}$$

obtained by sum over local open subsets U_i which covered T_θ, and sections chosen in each of them.

This expression has been used intensively for our numerical calculations.

Moreover, it can be shown (see e.g. [10],[6]) that:

$$\sum_{n=1}^{N} C_n = 1. \tag{21}$$

There is an alternative expression for C_n more suitable for our analytical calculations, given in eq. (27), (see [15] p.141). It is based on the motion of the zeros of the Bargmann representation of the states $|\varphi_n(\theta_1, \theta_2)>$.

5.2. **Chern indices of the semi-classical bands.** Our aim is to express the index C_n from the description of the classical dynamics.

Because of property (17), we deduce from theorem (1) page 22,that the band of the semi-classical spectrum $\sigma_{sc,t}$ have the same topology (and same Chern indices) as the actual energy bands.

Our work consists now in computing the index C_n of the semi-classical band n.

From theorem (6) page 25, the result is simply that:

$$C_n = I_n, \tag{22}$$

where I_n defined by eq. (19), is the homotopic number characterizing the path followed by the support of the quasi-mode on the cylinder, when θ_2 is varying from 0 to 2π.

5.3. **Global analysis of the Chern indices.** In this section we calculate the sum of Chern indices for consecutive bands, in order to recover the result eq.(21) within our semi-classical approach.

For each band $n = 1 \to N$, we have defined the cycle of the support $S_{T,n}$ on the torus T_{qp}, eq.(18). The last result eq.(22), is that the Chern index $C_n = I(S_n)$ is the homotopy number of this cycle (in the q direction). (We will now drop the T suffix in S_n).

We decide to define the sum of two or more consecutive cycles $S_n + S_{n+1} + \ldots + S_{n+a}$ by removing the jumping due to tunneling at the crossings between two consecutive cycles S_i and S_{i+1}. This is illustrated on figure 8. The homotopy is then $I(S_n + \ldots + S_{n+a}) = I(S_n) + \ldots + I(S_{n+a})$, because the removing is a local operation.

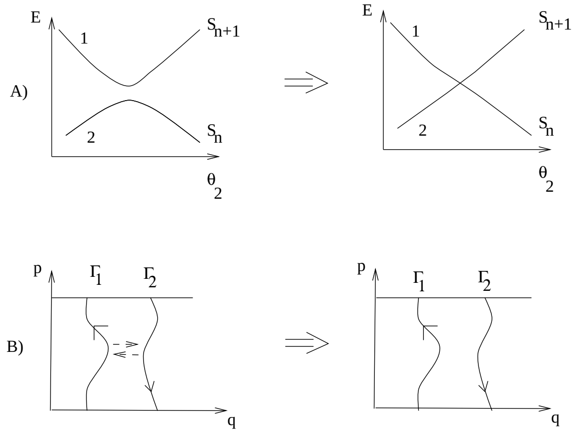

FIGURE 8. The tunneling effect generates a splitting between energy levels (A), and a jump of quasi-modes between trajectories (B). In order to calculate the sum $\sum_{n=1}^{N} C_n$, we have to remove this splitting, as well as this jump.

$\sum_{n=1}^{N} S_n$ is then the support of the semi-classical spectrum σ_{sc} without tunneling, and from proposition (2), it is composed of one cycle Γ_{nc} of homotopy 1 and many constant cycles $\Gamma_{c,i}$ of homotopy 0. This gives:

$$\sum_{n=1}^{N} C_n = \sum_{n=1}^{N} I(S_n) = I\left(\sum_{n=1}^{N} S_n\right) = +1.$$

We recover eq. (21). The total Chern index (+1) is interpreted here as the motion of the non contractible quasi-mode on the torus as θ_2 is varying (in accordance with th.6, page 25).

6. NUMERICAL ILLUSTRATION

We will illustrate the above results on the Hamiltonian eq.(3). The numerical calculations of the Chern indices have been done with the curvature formula eq.(20). For $N = 11$ levels, the Chern indices are:

$C_{1\to 4}$	C_5	C_6	C_7	$C_{8\to 11}$
0	+1	−1	+1	0

Our analytical results have been obtained in the $N \to \infty$ limit. Although, $N = 11$ is not very high, the numerical results which follow can well be interpreted in the semi-classical description of this paper.

The minimum value of N required to get correct semi-classical estimates, can be evaluated in the following manner: the mesh provided by Planck cells of magnitude $1/N$ has to be about so fine that all phase space structures in a plot like figure 1 can be resolved.

Figure 9, shows the energy levels $E_n(\theta_1, \theta_2)$ for $n = 1 \to 11$, as a function of θ_2. The dependence on θ_1 gives a width of the levels, but is very weak and not visible on the figure.

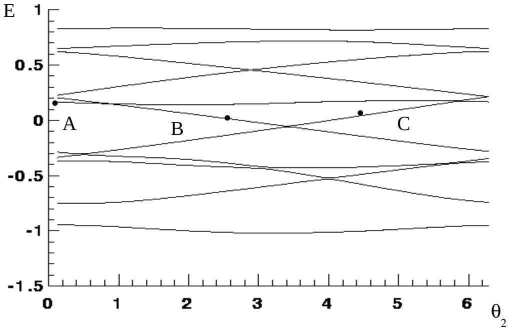

FIGURE 9. Energy levels $E_n(\theta_1, \theta_2)$ for $n = 1 \to 11$, of Hamiltonian eq.(3), as a function of θ_2. There is no degeneracy, but the small splittings are not visible on the figure. Points A,B,C, correspond to the Husimi representations of figure 11.

In this energy spectrum, one can clearly distinguish two categories of energy levels. These two categories are reproduced on figure 10, where we have artificially dropped the splittings. This figure corresponds to the semi-classical spectrum $\sigma_{sc}(\theta_2)$.

There are four energy levels (in solid line) which do not depend strongly on θ_2 and have periodicity 2π. In the light of prop. (2), these energy levels correspond to four quasi-modes $|\tilde{\psi}_c(\theta_2) >$ localized on contractible trajectories. There is also one continuous energy level $E_{nc}(\theta_2)$ (in dashed line) which depends on θ_2 and have periodicity $2\pi m$ with $m = 7$. This energy level corresponds to quasi-modes $|\tilde{\psi}_{nc}(\theta_2) >$ localized on non-contractible trajectories.

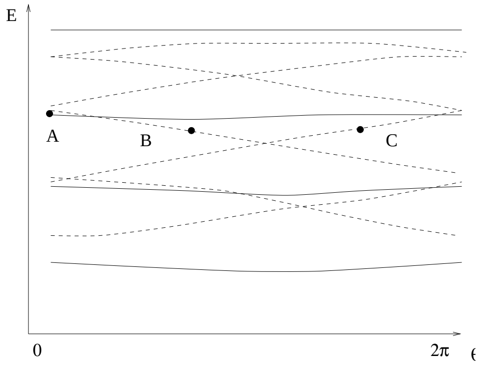

FIGURE 10. The semi-classical spectrum $\sigma_{sc}(\theta_2)$ obtained from fig.(9). The four solid lines correspond to quasi-modes $|\tilde{\psi}_c(\theta_2) >$ localized on contractible trajectories. The dashed line corresponds to quasi-modes $|\tilde{\psi}_{nc}(\theta_2) >$ localized on non-contractible trajectories.

Figure 11, shows the Husimi representation (see appendix (A)) of eigenstates $|\varphi_n(\theta_1, \theta_2) >$ for the level $n = 6$, with $\theta_1 = 0$, and three different values of θ_2. These three eigen-states correspond to the points A,B,C on figures (9) and (10). Looking at the classical trajectories on fig(1), one can clearly associate these quasi-modes respectively with the trajectories:

(A): with a contractible trajectory (point D on fig 1),
(B): a non-contractible trajectory of type $(0, +1)$,
(C): a non-contractible trajectory of type $(0, -1)$.

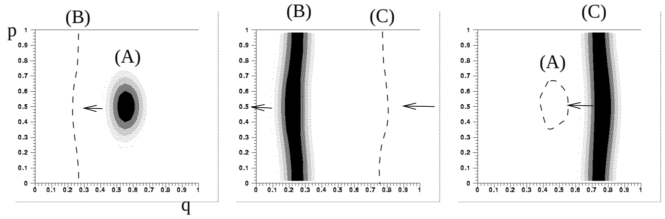

FIGURE 11. The dark density are the Husimi representation of eigenstates $|\varphi_n(\theta_1, \theta_2) >$ for the band $n = 6$ (see figure 9), with $\theta_1 = 0$, and three different values of θ_2. (A): $\theta_2 = 0$; (B): $\theta_2 = 2,5$, (C): $\theta_2 = 4,5$. The dashed lines are the trajectories where the quasi-modes will jump at the next crossing.

As θ_2 varies from 0 to 2π, the quantum state $|\varphi_6(\theta_1, \theta_2) >$ of level $n = 6$ jumps. From figure 9 and figure 10 it is evident that there are three (avoided) level crossings, where the quasi-mode jumps:

Now from figure 11, we can see that for the first crossing from (A) to (B), the quasi-mode stays in the same cell ($\Delta n_1 = 0$). For the second crossing from (B) to (C) the quasi-mode changes by $\Delta n_1 = -1$ cell. For the third crossing from (C) to (A), the quasi-mode stays in the same cell ($\Delta n_1 = 0$). This gives a total change of $\Delta n_1 = -1$ cell and a homotopy $I_6 = -1$ for this sequence of quasi-modes. Accordingly, we have $C_6 = I_6 = -1$. Our result eq.(22) is well verified here.

7. THE CHERN INDICES OF THE SPECTRUM IN A GENERIC SITUATION

From the above results, we give here the precise values of Chern indices for a simple and generic Hamiltonian (i.e. stable under perturbations) corresponding to the numerical example eq.(3) and explain how to read them from the Reeb graph (fig. 2).

To simplify the discussion, we suppose in this section that we deal with a Hamiltonian H such that the curve representing the non contractible trajectories in the Reeb graph, has only one maximum and minimum, like the dashed curve on fig. 2. We suppose moreover that in the energy range of this curve, there is only one family of contractible trajectories, like the solid line (C-D) on fig. 2.

In the range of energy of the non-contractible trajectories, each band of the spectrum is made with one of the three following sequences of quasi-modes, see figure (12):

- The band is made with the two non contractible trajectories of type $(0, \pm 1)$. This gives the sequence: $S = (+-)$.
- The band has also a quasi-mode on the contractible trajectory (c). This gives two possible sequences: $S = (c+-)$ or $S = (c-+)$.

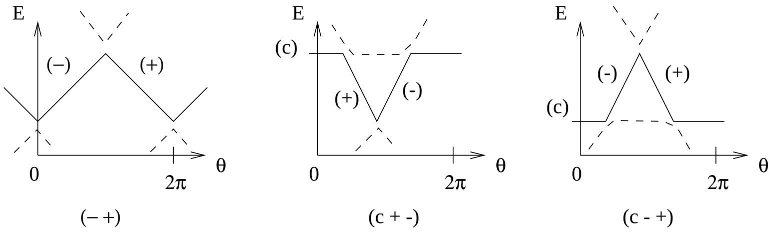

(− +)

(c + -)

(c - +)

FIGURE 12. The three possible band structures (solid lines), made with a non contractible trajectory of type $(0, \pm 1)$ and a contractible trajectory (c). The dashed lines are the upper and lower bands.

To simplify the discussion, we exclude sequences as $(c+c-)$ or $(c-c+)$. (These sequences do not appear if the energy intervals between successive energy levels of contractible quasi-modes are large enough).

It is clear from figure 12 that if the band n has the sequence $S_n = (c+-)$, then the band $n+1$ has necessary the sequence $S_{n+1} = (c-+)$, and conversely. These sequences come always by pair.

To illustrate this from our numerical example, we can see on figure (9) and figure (10), that the bands 3 to 9 have respectively the sequences: $S_3 = (c+-)$, $S_4 = (c-+)$,$S_5 = (+-)$,$S_6 = (c+-)$,$S_7 = (c-+)$,$S_8 = (+-)$, $S_9 = (+-)$.

Now we saw in prop. (3) that a non zero Chern index results from the jumping of neighboring quasi-modes on the cylinder, via non contractible trajectories. We saw also that a given quasi-mode $|\tilde{\psi}>$ jumps by tunneling effect to the nearest quasi-mode of the same energy located on a non contractible trajectory. It is therefore important to determine in which direction (right or left) this jump occurs: we have to complete the Reeb graph (fig 2), by giving the direction of the shortest jump between any two trajectory. For that purpose, it is sufficient to give the location of the separatrix between left-jumps and right-jumps.

On figure 13, we have reproduced the Reeb graph (the solid curve), and we have drawn (dashed line and dotted line) the possible location of this separatrix. The effect of this separatrix (dashed line) is shown with the plot of the jumps from one particular quasi-mode $|\tilde{\psi}>$ to a non-contractible trajectory of type (-1) at two different energies, on both sides of the separatrix. The separatrix for the jump from/to a non contractible of type $(+1)$ is in dotted line.

E_1 is the energy where this separatrix crosses the non-contractible trajectories family. That the energy E_1 is the same for the dashed and the dotted line comes simply from the reciprocity property of the tunneling "geodesic".

What matters in fact is only the intersection of this separatrix with the Reeb graph. The picture 13 is qualitative here, but quantitative calculations of the tunneling effect would precise the energy of these intersections.

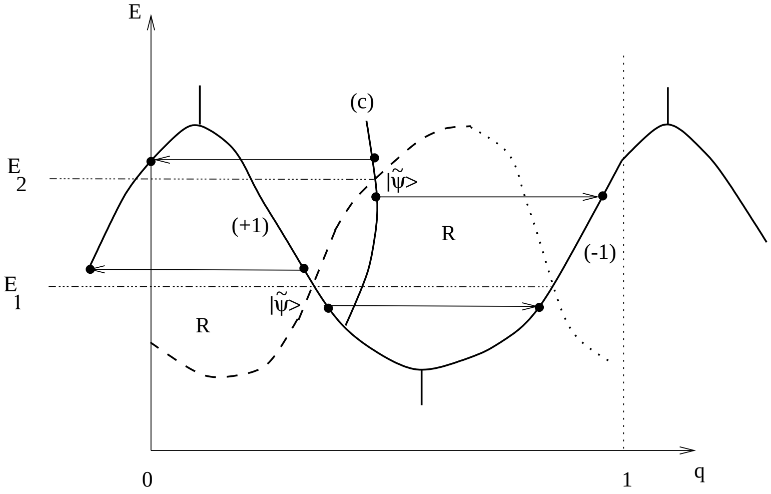

Figure 13. Example for the jumping of a quasi-mode $|\tilde{\psi}>$ to the nearest non contractible trajectory (of type $(0,-1)$). The solid curve is the Reeb graph as in fig. (2). The dotted and dashed lines represent the separatrix for these attraction basins.

Now, by combining figures 13 and 12 together with rule eq.(22), it is easy to compute the Chern index of the three kind of bands. This is done on figure 14 for the sequences S_5, S_6, S_8, and we infer the general result:

- If E_1 is in the range of a band of type $(+-)$ then its Chern index is $C_{(+-)} = +1$, otherwise $C_{(+-)} = 0$.
- If the trajectory (c) is in the region R (of fig. 13) then $C_{(c+-)} = -1$ (respect. $+1$), if the band has energy greater than E_1 (respect. lower). In the other regions, $C_{(c+-)} = 0$.
- If the trajectory (c) is in the region R then $C_{(c-+)} = +1$ (respect. -1), if the band has energy greater than E_1 (respect. lower). In the other regions, $C_{(c-+)} = 0$.

This allows us to interpret the Chern indices of our numerical example: the band $S_5 = (+-)$ with $C_5 = +1$ corresponds to the energy E_1. Above it, the two bands S_6,S_7 with Chern indices $C_6 = -1$, $C_7 = +1$ form a pair, thanks to the presence of the contractible trajectory (c) in region R.

As a general result, we conclude that for any choice of Hamiltonian H with a similar Reeb graph, there is a unique band in the middle of the spectrum, including

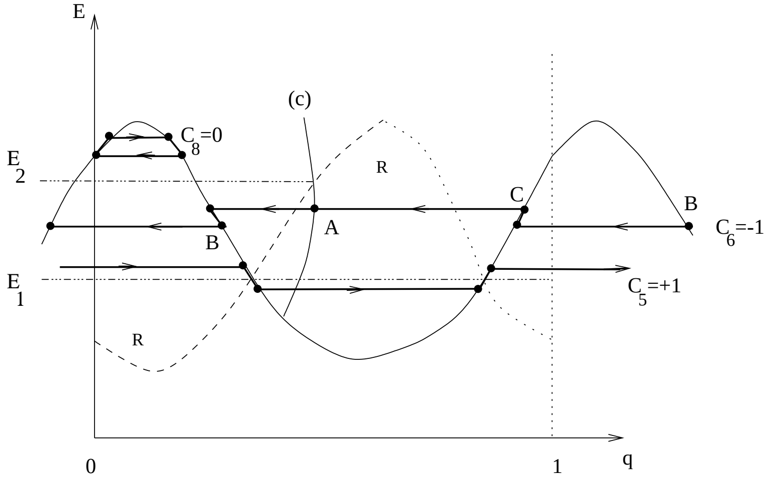

FIGURE 14. From knowledge of the sequences S_5, S_6, S_8, their homotopy and the Chern indices $C_5 = +1$, $C_6 = -1$ and $C_8 = 0$ are graphically computed. $C_5 = +1$ is associated with a band of energy E_1. Note that $C_6 = -1$ is non zero thanks to the quasi-mode (A) on the contractible trajectory (c) in region R.

energy E_1, with Chern index $+1$. Above this energy (for $E_1 < E < E_2$), the Chern indices come by pairs $(-1, +1)$, and under the energy E_1, the Chern indices come by pairs $(+1, -1)$.

Of course for another appearance of the Reeb graph, the rules could be different. In particular, the Chern indices can reach higher values if the non-contractible curve of the Reeb graph has more than one maximum. We do not know if there a simple and explicit expression of the Chern indices in the general case.

8. CHERN INDEX AND HALL CONDUCTIVITY

It is well known [1] that the Chern index C of a band is related to the transverse Integer Quantum Hall conductivity σ_{xy} by the relation eq.(1). The usual demonstration of this formula starts from the Kubo linear response formula for σ_{xy}, and expresses it as the curvature integral for C, eq.(20). In this section we want to demonstrate it from an other point of view, by relating C with the motion of a wave packet on the plane T_{qp}. This result seems more intuitive.

Consider a given energy band n of the spectrum eq.(11). For each (θ_1, θ_2) there is one eigenvector $|\varphi_n(\theta_1, \theta_2)>$ defined up to a multiplicative constant. Suppose that we have a C^∞ function $(\theta_1, \theta_2) \rightarrow |\psi(\theta_1, \theta_2)> \in \mathcal{H}_T(\theta_1, \theta_2)$, where $|\psi(\theta_1, \theta_2)>$ is proportional to $|\varphi_n(\theta_1, \theta_2)>$, eq.(11). Note that if $C_n \neq 0$, this function must be zero at some values of (θ_1, θ_2).

Consider now

$$|\psi>= \int\int d\theta_1 d\theta_2 |\psi(\theta_1, \theta_2)> .$$

Then $|\psi> \in \mathcal{H}_P = L^2(I\!R)$. We can say that $|\psi>$ is a state "localized" on the plane T_{qp} constructed from the band n, like Wannier states in Solid State Physics. (Conversely, given $|\Phi> \in L^2(I\!R)$, we can project it on the spectral band n and obtain such $|\psi>$.)

The state $|\psi>$ can be translated by (n_1, n_2) cells on the plane by:

$$|\psi_{n_1,n_2}>= T_Q^{n_1} T_P^{n_2} |\psi>= \int\int d\theta_1 d\theta_2 e^{in_1\theta_1 + in_2\theta_2} |\psi(\theta_1, \theta_2)> .$$

Conversely:

$$|\psi(\theta_1,\theta_2)>=\sum_{n_1,n_2\in\mathbb{Z}^2} e^{-in_1\theta_1-in_2\theta_2}|\psi_{n_1,n_2}> .$$

These simple relations can be generalized by the following result:

Consider an other state constructed from the band n:

$$|\phi>=\int\int d\theta_1 d\theta_2 e^{if(\theta_1,\theta_2)}|\psi(\theta_1,\theta_2)>, \tag{23}$$

where f is a continuous and periodic function such that:

$$f(\theta_1+2\pi,\theta_2)=f(\theta_1,\theta_2)+N_1 2\pi$$
$$f(\theta_1,\theta_2+2\pi)=f(\theta_1,\theta_2)+N_2 2\pi,$$

($N_1,N_2\in\mathbb{Z}^2$ are topological integers which characterized the homotopy of the function f).

Let us define:

$$<n_1>=\sum_{n_1,n_2} n_1.\left|<\psi_{n_1,n_2}|\phi>\right|^2$$
$$<n_2>=\sum_{n_1,n_2} n_2.\left|<\psi_{n_1,n_2}|\phi>\right|^2 ,$$

which give the mean position of the state $|\phi>$on the plane T_{qp} relatively to the localized states $|\psi_{n_1,n_2}>$. It is easy to prove that:

$$<n_1>=N_1$$
$$<n_2>=N_2,$$

the mean position of $|\phi>$is then “quantized”.

(This is a simple property of Fourier series: if $g(\theta)=\sum_n c_n e^{in\theta}=e^{if(\theta)}$ is periodic and $f(2\pi)=f(0)+N2\pi$ then $N=\sum_n n|c_n|^2$. Another way to say it is: $\sum_n n|c_n|^2=<g|\hat{p}_\theta|g>=\frac{1}{2\pi}\int_0^{2\pi} f' d\theta=N$, with the current operator $\hat{p}_\theta=\frac{1}{i}d/d\theta$.).

We now give some consequences of this result on the “quantized mean position”.

Now let us first look at the time evolution of $|\psi_{0,0}>$:

$$|\psi(t)>=e^{-iHt/\hbar}|\psi_{0,0}>=\int\int d\theta_1 d\theta_2 e^{-iE(\theta_1,\theta_2)t/\hbar}|\psi(\theta_1,\theta_2)> .$$

Comparing to eq.(23), the phase function is the dynamical phase $f(\theta_1,\theta_2)=-E(\theta_1,\theta_2)t/\hbar$ of homotopy type $N_1=N_2=0$. (because by continuous homotopy $t\to 0$, f is mapped to 0). This means that during its evolution, the quantum state $|\psi(t)>$spreads over the plane, but its mean position $<n_1>$,$<n_2>$ stays zero.

Let us suppose now that θ_1,θ_2 are no more “good quantum numbers”, and that there is a slow drift. In the model of bi-dimensional electrons of the introduction, this drift is the adiabatic motion due to the low electrical field E_x. Consider for example:

$$\theta_1(t)=-\omega_1 t$$
$$\theta_2(t)=\theta_2(0).$$

After one period $T=2\pi/\omega_1$, the evolution gives

$$e^{-iHT/\hbar}|\psi(\theta_1,\theta_2)>=\exp\left(i\phi_D(\theta_1,\theta_2)+i\phi_B(\theta_2)\right)|\psi(\theta_1,\theta_2)>,$$

where $\phi_D(\theta_1,\theta_2)$ is the dynamical phase of homotopy type $N_1=N_2=0$ and $\phi_B(\theta_1,\theta_2)$ is the Berry's phase of the path $\theta_1(t)$ and doesn't depend on θ_1 henceforth. By homotopy deformation, $\phi_B(\theta_2)\equiv 2\pi C\theta_2$ and is therefore of type $N_1=0$, $N_2=C$. This means that after one period T, the mean position of the quantum state $|\psi(t)>$has been changed by $\delta<n_1>=0$, $\delta<n_2>=C$ (in cells units).

This "quantized" velocity $V_2 = \delta < n_2 > /T$ is responsible for the Integer Hall conductivity. Indeed, in the Harper Model [1] of non interacting bi-dimensional (x, y) electrons in a bi-periodic potential of period (X, Y), and a perpendicular high magnetic field B_z, with a low electrical field along E_x, the adiabatic hypothesis gives:

$$\theta_1(t) = -\frac{eX}{\hbar} E_x t.$$

We have obtained that the quantized velocity of one electron quantum state is $V_y = (CY)/T$. For a filled band, the electronic density is one electron per cell: $\rho = 1/(XY)$. The electronic density current of a filled band is then $j_y = \rho e V_y = \frac{e^2}{h} C.E_x$ which leads to eq.(1).

9. Conclusion

By using quasi-modes, we have obtained a semi-classical description of band eigen-states of a generic quantum Hamiltonian on the torus phase-space. By using general results exposed in the appendices, relating the topological Chern index of a band, with the localization properties of the quantum states, we have been able to express the Chern index of each band in terms of the motion of the quasi-modes on the classical phase space.

In section 7, we have shown how the Chern indices of the whole spectrum can be graphically computed from the classical Reeb graph. There is an interesting question which can be raised from our work: conversely, from a given sequence $(C_n)_n$ of integers such that $\sum_n C_n = +1$, the question would be to determine the potential $V(x, y)$ whose band spectrum possess this precise sequence of Chern indices.

Currently one tries to observe experimental signatures of the Harper spectrum (Landau level substructures) in superlattices with periods of about 100 nm on GA-As-AlGaAs heterojunctions ([27],[28]). In these experiments, the Chern index gives the quantum Hall conductivity σ_{xy}. In this paper we have shown simple correspondances between the Chern index and the classical trajectories of the electrons. This correspondances could be observed in experiments by measuring the variations of the integer Hall conductivity, in relation with the potential $V(x, y)$ of the supperlattice, which may be created by an external electrostatic grid.

10. Acknowledgments

Discussions with B. Parisse and Y. Colin de Verdiere are gratefully acknowledged.

Appendix A. Bargmann and Husimi representation

In this appendix, we recall well known results on Bargmann and Husimi representation on the torus phase space ([19]).

We have seen previously that the space $\mathcal{H}_T$ is not a subspace of $L^2(\mathbb{R})$. For functions belonging to $\mathcal{H}_T$, it will be more useful to introduce a phase space representation of the quantum states, called the Bargmann representation ([29]).

Consider a quantum state $|\psi> \in L^2(\mathbb{R})$. In order to characterize the localization of $|\psi>$ in the phase space near the point (q, p), we first construct a Gaussian wave packet $|qp>$ (coherent state) defined in the x-representation by:

$$< x|qp >= \left(\frac{1}{\pi\hbar}\right)^{1/4} \exp(\frac{i}{\hbar} px) \exp(-\frac{(x-q)^2}{2\hbar}).$$

The notation $|qp>$ recalls that the coherent state is localized (in the semi-classical limit) at the point (q, p) of the phase space.

The Husimi distribution of a state $|\psi>$ is defined over the phase space by:

$$h_\psi(q,p) = |<qp|\psi>|^2,$$

and for $\varphi \in L^2(I\!\!R)$, we have:

$$\int |\varphi(x)|^2 \; dx = \int\int |<qp|\varphi>|^2 \; \frac{dq\; dp}{2\pi\hbar}. \tag{24}$$

To characterize the functions of $L^2(T^*I\!\!R)$ which are (q,p) representations of a state, it is more convenient to introduce a complex representation of the phase space $z = \frac{1}{\sqrt{2\hbar}}(q+ip)$. Another (proportional) expression of the coherent state is then:

$$|z>= \exp(za^+)|0>,$$

with $|0>$ being the fundamental of the harmonic oscillator $H_0 = \hat{q}^2 + \hat{p}^2$, and a^+ being the associated creation operator. Indeed:

$$|qp>= \exp(i\frac{qp}{2\hbar} - \frac{q^2+p^2}{4\hbar})|z> .$$

The following anti-holomorphic function of z is called the Bargmann distribution of ψ:

$$b_\psi(z) =< z|\psi> .$$

Clearly, we have

$$h_\psi(q,p) = |b_\psi(z)|^2 \, e^{-\frac{q^2+p^2}{2\hbar}},$$

hence the zeroes of the function $h_\psi(q,p)$ are those of the holomorphic function $b_\psi(z)$, which are localized zeroes in the phase space. Moreover, (24) implies that $\psi \in L^2(I\!\!R)$ if and only if $b_\psi \in L^2(\mathbb{C}, e^{-|z|^2/h})$ and b_ψ is anti-holomorphic.

The same definitions can be applied for a state $|\psi>\in \mathcal{H}_T(\theta_1,\theta_2)$. The corresponding Bargmann function is a theta-function [30] and the Husimi distribution is bi-periodic in (q,p), hence is well defined on the torus T_{qp}.

We need the following properties concerning the Bargmann representation $b_\psi(z) =< z|\psi>$ of a quantum state $|\psi>$ on the torus ($|z>$ is a coherent state on the torus [31]:

If $|\psi>\in \mathcal{H}_T(\theta_1,\theta_2)$, the Bargmann function $b_\psi(z)$ is (a theta-function) anti-holomorphic with respect to z, and with N zeros $Z = (z_1;\ldots,z_N)$ in the cell $[0,1]\times[0,1]$. These zeros are constrained by ([30], this is “Abel theorem”, and “Jacobi inversion theorem”, see [15] p.235):

$$\sum_{i=1}^{N} q_i = \frac{\theta_2}{2\pi} \tag{25}$$
$$\sum_{i=1}^{N} p_i = \frac{\theta_1}{2\pi}.$$

with $z_i = q_i + ip_i$. Conversely, such a collection of N zeros define a state $|\psi>\in \mathcal{H}_T(\theta_1,\theta_2)$, unique up to a multiplicative constant.

Note that since the N zeroes are constrained to have a fixed sum, we get the right dimension $N-1+1$ for the Hilbert space $\mathcal{H}_T(\theta_1,\theta_2)$.

Appendix B. Calculation of the Chern index in special cases

For simplicity, we will note $\theta = (\theta_1,\theta_2) \in I\!\!R^2$.

We will compute the Chern index of a line bundle in particular cases. We will always consider a line sub-bundle of $\mathcal{H}_T(\theta) \to T_\theta$. Such a line bundle F is characterized by giving local section $\theta \to |\psi_i(\theta)>\in \mathcal{H}_T(\theta)$ over open sets U_i which cover T_θ.

From appendix A, the line bundle F is also characterized by the function $\theta \to Z(\theta)$, where $Z(\theta)$ is the set of N non-ordered zeroes of the Bargmann functions $b_{\psi(\theta)}(z)$.

B.1. Theorem on homotopy invariance.

Theorem 1. . *Consider two complex line bundles over T_θ with Chern index C and C' defined by local sections $|\psi_i(\theta)>$and $|\psi'_i(\theta)>$on open sets U_i. Suppose moreover that*

$$<\psi_i(\theta)|\psi'_i(\theta)>\neq 0, \quad \forall\theta,\ \forall i,$$

then $C = C'$.

Proof. We can suppose that the sections are normalized ($<\psi_i(\theta)|\psi_i(\theta)>=1$). On a set U_i, and for a given θ, define:

$$\rho_i(\theta) = |<\psi_i(\theta)|\psi'_i(\theta)>| \leq 1,$$

and for fixed $\lambda \in [0,1]$:

$$|\varphi_{i,\lambda}(\theta)>=|\psi_i(\theta)>.<\psi_i(\theta)|\psi'_i(\theta)>+\lambda\left(|\psi'_i(\theta)>-|\psi_i(\theta)><\psi_i(\theta)|\psi'_i(\theta)>\right).$$

In the theorem, we suppose that $\rho_i(\theta) > 0$. Thus

$$<\psi'_i(\theta)|\varphi_{i,\lambda}(\theta)>=\rho^2+\lambda(1-\rho^2)>0,$$

and then $|\varphi_{i,\lambda}(\theta)>\neq 0$.

We now check that the sections $|\varphi_{i,\lambda}(\theta)>$ define a complex line bundle F_λ. On an other set U_j, if $|\psi_j(\theta)>=\exp(i\alpha)\ |\psi_i(\theta)>$and $|\psi'_j(\theta)>=\exp(i\beta)\ |\psi'_i(\theta)>$ then $|\varphi_{j,\lambda}(\theta)>=\exp(i\beta)\ |\varphi_{i,\lambda}(\theta)>$ is in the same line than $|\varphi_{i,\lambda}(\theta)>$.

We have thus obtain a homotopic deformation F_λ, $\lambda \in [0,1]$ between the line bundle F_0 and F_1. They have thus the same Chern index $C = C_\lambda = C'$. ☐

Theorem 2. *More generally ([15],p. 141) if we suppose that*

$$\theta \to <\psi_i(\theta)|\psi'_i(\theta)>,$$

has zeros in θ^* with index $\iota(\theta^*) = \pm 1$,then

$$C = C' + \sum_{zeros\ \theta^*} \iota(\theta^*). \tag{26}$$

B.2. The Chern index from the zeroes of the Bargmann function.

Let F be a line bundle as above.

- Suppose that there exists some point $z_0 \in T_{qp}$ of phase space, such that

  $$\forall\theta \in T_\theta, \quad b_{\psi(\theta)}(z_0) \neq 0,$$

  (equivalently, this means that $z_0 \notin Z(\theta)$, for all θ). Then we can select a vector $|\psi(\theta)>\in H_N(\theta)$ in each fiber such that $\arg\left(b_{\psi(\theta)}(z_0)\right) = 0$. This gives a non-vanishing global section of the bundle. This is also a global frame, hence the bundle is trivial, and $C = 0$.
- More generally, define

  $$N(z_0) = \{\theta \in T_\theta \quad / \quad z_0 \in Z(\theta)\},$$

  then

  $$C = \sum_{\theta \in N(z_0)} (\pm 1), \tag{27}$$

  where the sign ± 1 corresponds to the local orientation of the mapping z_i at θ, where $Z = \{z_1, \dots, z_N\}$ and $z_i(\theta) = z_0$. This can be deduced directly from eq.(26), with $|\psi'>=|z_0>$.

B.3. **Example of a line bundle with a given Chern index C.** We now construct explicit examples of such a bundle.

- Suppose that $N \geq 2$. We define a line bundle F_0, by specifying the zeros of the Bargmann representation of a section, with the notations of eq.(25):

$$q_1 = \frac{\theta_2}{2\pi}, \quad p_1 = 0 \tag{28}$$

$$q_2 = 0, \quad p_2 = \frac{\theta_1}{2\pi}$$

$$q_i = 0, \quad p_i = 0 \text{ for } 3 \leq i \leq N.$$

  The constraint eq.(25) is easily verified. If we choose $z_0 = (q_0 + ip_0)$ with $q_0 = p_0 = 0.5$, $z_0 \notin Z(\theta)$ and from eq. (27), we deduce that the bundle F_0 is trivial, with Chern index $C = 0$.
- More generally, consider the bundle F_C defined by

$$q_1 = (1-C)\frac{\theta_1}{2\pi}, \quad p_1 = 0$$

$$q_2 = C\frac{\theta_2}{2\pi}, \quad p_2 = \frac{\theta_1}{2\pi}$$

$$q_i = 0, \quad p_i = 0 \quad \text{for } 3 \leq i \leq N.$$

  The constraint eq.25 is verified. We can apply eq. (27), to calculate the Chern index C . The set $N(z_0)$ is given by

$$\theta_1 = \pi\ [2\pi], \quad \theta_2 = \frac{\pi}{C}\ [2\pi/C],$$

  and we obtain that the Chern index is C.

B.4. **Chern index for a moving coherent state.**

Theorem 3. *Suppose $N \geq 2$. Consider the line bundle F_z defined by the local section $|\psi(\theta)>=|z_\theta>\in \mathcal{H}_T(\theta)$ with $z_\theta = q_\theta + ip_\theta$, and*

$$\begin{pmatrix} q_\theta \\ p_\theta \end{pmatrix} = \begin{pmatrix} n_{11} & n_{12} \\ n_{21} & n_{22} \end{pmatrix} \begin{pmatrix} \theta_1/2\pi \\ \theta_2/2\pi \end{pmatrix}, \tag{29}$$

(This means that the coherent state $|z_\theta>$ is moving over the cells as θ is varying.) The Chern index of this bundle is then

$$C = N. \begin{vmatrix} n_{11} & n_{12} \\ n_{21} & n_{22} \end{vmatrix} + n_{21} + n_{12}. \tag{30}$$

Proof. Consider the line bundle F_0 defined by the zeroes eq.(28), with local section noted $|\varphi_i(\theta)>$ on each open set $U_i \subset T_\theta$. This bundle has $C = 0$ Chern index. Consider the function

$$f : \theta \to <\varphi_i(\theta)|z_\theta> .$$

From eq.(26), the Chern index C of the bundle F_z is

$$C = \sum_{\theta^* \text{zeroes of f}} \iota(\theta^*).$$

The zeroes of f are given by:

$$<\varphi_i(\theta)|z_\theta>=0 \quad \Leftrightarrow \; z_\theta \text{ is a zero of the section } |\varphi_i(\theta)>$$

$$\Leftrightarrow \left\{ \begin{array}{l} q_\theta = q_i \\ p_\theta = p_i \end{array} \right. , i = 1, \ldots, N.$$

this gives

$$\left\{ \begin{array}{l} n_{11}\frac{\theta_1}{2\pi} + n_{12}\frac{\theta_2}{2\pi} \\ n_{21}\frac{\theta_1}{2\pi} + n_{22}\frac{\theta_2}{2\pi} \end{array} \right. = \left\{ \begin{array}{c} \frac{\theta_2}{2\pi} \\ 0 \end{array} \right. \text{ or } = \left\{ \begin{array}{c} 0 \\ \frac{\theta_1}{2\pi} \end{array} \right. \text{ or } = \left\{ \begin{array}{c} 0 \\ 0 \end{array} \right. \text{for } i = 3, \ldots, N.$$

We deduce from eq.(2) that

$$\begin{aligned} C = & \left| \begin{array}{cc} n_{11} & n_{12}-1 \\ n_{21} & n_{22} \end{array} \right| + \left| \begin{array}{cc} n_{11} & n_{12} \\ n_{21}-1 & n_{22} \end{array} \right| + (N-2) \left| \begin{array}{cc} n_{11} & n_{12} \\ n_{21} & n_{22} \end{array} \right| \\ = & \quad N \left| \begin{array}{cc} n_{11} & n_{12} \\ n_{21} & n_{22} \end{array} \right| + n_{21} + n_{12}. \end{aligned}$$

□

B.5. **Bundle constructed from periodic motion of states on the plane.** A natural question is : is it possible to generalize the theorem 3, for the periodic motion of arbitrary states in $L^2(I\!\!R)$ rather than only coherent states?

There is a first result:

Theorem 4. *Let $S : \theta \to |\psi(\theta)> \in L^2(I\!\!R)$ for $\theta \in I\!\!R^2$ be an arbitrary mapping such that :*

$$\forall \theta, \quad |\psi(\theta)> \neq 0 \tag{31}$$
$$|\psi(\theta_1 + 2\pi, \theta_2)> = T_Q^{n_{11}} T_P^{n_{12}} |\psi(\theta)>$$
$$|\psi(\theta_1, \theta_2 + 2\pi)> = T_Q^{n_{21}} T_P^{n_{22}} |\psi(\theta)> \quad .$$

with $(n_{11}, n_{12}, n_{21}, n_{22}) \in Z\!\!\!Z^4$ which characterizes the periodic motion of the states $|\psi(\theta)>$ as θ is varied.

For a contractible open subset U of T_θ, define

$$|\tilde{\psi}(\theta)> = P_{\theta_1} P_{\theta_2} (|\psi(\theta)>) \in \mathcal{H}_T(\theta).$$

Then if $N \geq 3$, and for a generic map S, $|\tilde{\psi}(\theta)>$ gives a local section of a well defined line bundle over T_θ, which can be noted also S.

Proof. For every θ, the line bundle is defined by the vector $|\tilde{\psi}(\theta)>$. We have therefore to check that $|\tilde{\psi}(\theta)> \neq 0$, and that this line is periodic with respect to θ.

Because the space $\mathcal{H}_T(\theta)$ is N dimensional, the condition $|\tilde{\psi}(\theta)> = 0$ is N-dimensional. As soon as $N > 2$, and for $\theta \in [0, 2\pi]^2$the condition $|\tilde{\psi}(\theta)> = 0$ cannot be satisfied generically. Now

$$\begin{aligned} |\tilde{\psi}(\theta_1 + 2\pi, \theta_2)> &= P_{\theta_1 + 2\pi}(|\psi(\theta_1 + 2\pi)>) \\ &= P_{\theta_1} T_Q^{n_{11}} T_P^{n_{12}} |\psi(\theta_1)> \\ &= \exp(i n_{11} \theta_1) \exp(i n_{12} \theta_2) |\tilde{\psi}(\theta)> . \end{aligned}$$

So $|\tilde{\psi}(\theta)>$ and $|\tilde{\psi}(\theta_1 + a2\pi, \theta_2 + b2\pi)>$are proportional and define the same line $\forall (a, b) \in Z\!\!\!Z^2$. □

Theorem 5. *Suppose that $N \geq 4$. Let $S : \theta \to |\psi(\theta)> \in L^2(I\!\!R)$ be a generic mapping as defined in theorem 4a. Then the Chern index of the line bundle S is given by formula (30).*

Proof. We note $S_0 = S$, and $S_1 = F_z$ the line bundle defined in theorem 3. The proof consists in constructing a homotopic deformation S_λ from S_0 to S_1 for $\lambda \in [0, 1]$. Because the Chern index C_λ of S_λ is constant, we therefore conclude that the Chern index of S is given by formula (30).

For $\lambda \in [0, 1]$, and $\theta \in I\!\!R^2$, define

$$|\psi_\lambda(\theta)> = \lambda |\psi(\theta)> + (1 - \lambda)|z(\theta)> \in L^2(I\!\!R),$$

where $|z(\theta)>$ is a standard coherent state on the plane, $z(\theta) = q_\theta + i p_\theta$, with q_θ, p_θ given by eq. (29). We suppose moreover that the phases are chosen such that eq. (31) holds for $|z(\theta)>$ and $|\psi(\theta)>$.

Then $|\psi_\lambda(\theta)> = 0$ if and only if $\lambda = 1/2$ and $|\psi(\theta)> = -|z(\theta)>$. This last situation is non generic, and if it occurs, we can just choose $z(\theta) = (q_\theta + q_0) +$

$i(p_\theta + p_0)$ with arbitrary q_0, p_0 to avoid this. So $S_\lambda : \theta \to |\psi_\lambda(\theta) >\in L^2(I\!R)$ fulfills theorem 4, and defines a line bundle for every λ. Because there are three parameters $\theta_1, \theta_2, \lambda$ we have to suppose now that $N \geq 4$ so that $|\tilde{\psi}(\theta) >\neq 0$. □

B.6. **Bundle constructed from a periodic motion on the cylinder.** In section 4, we obtain the periodic motion of quasi-modes on the cylinder C_{qp} phase-space. A slightly different result than theorem 5 is then needed:

Theorem 6. *Suppose* $N \geq 4$, *and let*

$$\theta_2 \in I\!R \to |\psi_C(\theta_2) >\in \mathcal{H}_C(\theta_2),$$

be a generic continuous mapping such that

$$\forall \theta_2 \in I\!R, \qquad |\psi_C(\theta_2) >\neq 0,$$
$$|\psi_C(\theta_2 + 2\pi) >= T_Q^I |\psi_C(\theta_2) >,$$

with $I \in Z\!\!Z$.

For $\theta = (\theta_1, \theta_2)$ *define*

$$|\tilde{\psi}(\theta) >= P_{\theta_1} |\psi_C(\theta_2) >\in \mathcal{H}_T(\theta).$$

Then $\theta \to |\tilde{\psi}(\theta) >\in \mathcal{H}_T(\theta)$ *is a local section of a well defined line bundle over* T_θ, *with Chern index* I.

Proof. The proof is similar to that of theorem 5.

The bundle is well defined because, first $|\tilde{\psi}(\theta) >= 0$ needs N conditions, generically not realized for arbitrary $\theta_1, \theta_2 \in [0, 2\pi]$, as soon as $N > 2$.

Secondly, $|\tilde{\psi}(\theta) >$ and $|\tilde{\psi}(\theta_1 + a2\pi, \theta_2 + b2\pi) >= P_{\theta_1} T_Q^{Ib} |\psi_C(\theta_2) >= \exp(iIb\theta_1)|\tilde{\psi}(\theta) >$ are proportional and define therefore the same line.

In order to calculate the Chern index, consider the mapping

$$\theta_2 \in I\!R \to |z(\theta_2) >\in L^2(I\!R),$$

where $|z(\theta_2) >$ is a standard coherent state on the plane, $z(\theta_2) = q_\theta + ip_\theta$, and

$$q_\theta = I.\theta_2$$
$$p_\theta = p_0 = constant,$$

we can therefore construct $|z(\theta_2)_C >= P_{\theta_2} |z(\theta_2) >\in \mathcal{H}_C(\theta_2)$ and $|z(\theta_1, \theta_2) >= P_{\theta_1} |z(\theta_2)_C >\in \mathcal{H}_T(\theta)$.

From theorem 3, $\theta \to |z(\theta_1, \theta_2) >$ define a line bundle with Chern index $n_{12} = I$.

Consider now for $\lambda \in [0, 1]$

$$\theta_2 \to |\psi_\lambda(\theta_2) >= \lambda |\psi(\theta_2) > + (1 - \lambda)|z(\theta_2)_C >\in \mathcal{H}_C(\theta_2),$$

and

$$S_\lambda : \theta = (\theta_1, \theta_2) \to |\tilde{\psi}_\lambda(\theta) >= P_{\theta_1} |\psi_\lambda(\theta_2) >\in H_T(\theta).$$

Then for fixed λ, S_λ define a line bundle over T_θ, because $|\tilde{\psi}_\lambda(\theta) >= 0$ nor $|\psi_\lambda(\theta) >= 0$ are generic (cf discussion in proof of theorem 5), and there is also periodicity with respect to θ.

The mapping $\lambda \to S_\lambda$ is a homotopic deformation from the line bundle $\theta \to |\tilde{\psi}(\theta) >$ to the line bundle $\theta \to |z(\theta_1, \theta_2) >$. Their Chern index is constant and equal to I.

□

References

[1] D. J. Thouless, M. Khomoto, M. P. Nightingale, and M. den Nijs. Quantized hall conductance in a two-dimensional periodic potential. *Phys. Rev. Lett.*, 49, 1982.

[2] B. Simon. Holonomy, the quantum adiabatic theorem and berry's phase. *Phys. Rev. Lett.*, 51, 1983.

[3] Jean Bellissard and A. van Elst and H. Schulz-Baldes. The noncommutative geometry of the quantum Hall effect. *J. Math. Phys.*, 35 (10):5373–5451, 1994.

[4] D. Thouless. "Topological interpretations of quantum Hall conductance.". *J. Math. Phys.*, 35 (10):5362–5372, 1994.

[5] Yves Colin de Verdière. Fibrés en droites et valeurs propes multiples. *Séminaire de théorie spectrale -Institut Fourier Grenoble*, pages 9–18, 92-1993.

[6] J. E. Avron, R. Seiler, and B. Simon. Homotopy and quantization in condensed matter physics. *Phys. Rev. Lett.*, 51, 1983.

[7] D. Springsguth, R. Ketzmerick, and T. Geisel. Hall conductance of bloch electrons in a magnetic field. *Phys. Rev. B*, 56:2036, 1997.

[8] Arnol'd, V.I. Modes and quasimodes. *Funct. Anal. Appl.*, 6:94–101, 1972.

[9] Lazutkin, Vladimir F. *KAM theory and semiclassical approximations to eigenfunctions. With an addendum by A. I. Shnirelman.* Springer-Verlag, 1993.

[10] D. P. Arovas, P. N. Bhatt, F. D. M. Haldane, P. B. Littlewood, and R. Rammal. Localization, wave function topology, and the integer quantized hall effect. *Phys. Rev. Lett.*, 60, 1988.

[11] F. Faure. Generic description of the degeneracies in Harper-like models. *J. Phys. A, Math. Gen.*, 27 (22):7519–7532, 1994.

[12] F. Faure,B. Parisse. Semiclassical study of the origin of quantized Hall conductance in periodic potentials. *Submitted to JMP*, 1998.

[13] Dufour, Jean-Paul and Molino, Pierre and Toulet, Anne. Classification des systemes integrables en dimension 2 et invariants des modeles de Fomenko. (Classification of integrable systems on two-dimensional manifolds and invariants in Fomenko's models). *C. R. Acad. Sci., Paris, Ser. I 318*, 10:949–952, 1994.

[14] Milnor, J. *Morse theory. Based on lecture notes by M. Spivak and R. Wells*, volume VI. 1963.

[15] Griffiths, Phillip and Harris, Joseph. *Principles of algebraic geometry.* A Wiley-Interscience Publication. New York, 1978.

[16] Bernard Helffer and Johannes Sjöstrand. Multiple wells in the semi-classical limit-I. *Communication in Partial Differential Equation*, 9(4):337–408, 1984.

[17] M. Wilkinson. Critical properties of electron eigenstates in incommensurate systems. *Proc. R. Soc. Lond. A*, 391, 1984.

[18] M. Wilkinson and E.J. Austin. Phase space lattices with threefold symmetry. *J. Phys. A*, 23, 1990.

[19] A. Voros. Wentzel-kramers-brillouin method in the bargmann representation. *Phys. Rev. A*, 40, 1989.

[20] M. Saraceno J. Kurchan, P. Leboeuf. Semiclassical approximation in the coherent state representation. *Phys. Rev. A*, 40, 1989.

[21] T. Paul and A Uribe. A construction of quasi-modes using coherent states. *Ann. Inst. H. Poincaré, Phys. théor*, 59 (4):357–381, 1993.

[22] Yves Colin de Verdière and B. Parisse. Équilibre instable en régime semi-classique - I. Concentration microlocale. *Communications in Partial Differential Equations*, 19(9-10):1535–1563, 1994.

[23] Yves Colin de Verdière and B. Parisse. Équilibre instable en régime semi-classique - II. Conditions de Bohr-Sommerfeld. *Annales de l'Institut Henri Poincaré- Physique Théorique*, 61(3):347–367, 1994.

[24] Yves Colin de Verdière and B. Parisse. Les conditions de Bohr-Sommerfeld singulières. *Preprint de l'Institut Fourier, Grenoble*, 432, 1998.

[25] Avron, J.E. and Sadun, L. and Segert, J. and Simon, B. Chern numbers, quaternions, and Berry's phases in Fermi systems. *Commun. Math. Phys.*, 124, No 4:595–627, 1989.

[26] M.V. Berry. Quantal phase factors accompanying adiabatic changes. *Proc. Roy. Soc. Lond.*, 45, 1984.

[27] V. Gudmundsson and R.R. Gerhardts. *Phys. Rev. B*, 54:5223, 1996.

[28] T. Schlosser, K. Ensslin, J.P. Kotthaus, and M. Holland. *Europhys. Lett.*, 33:683, 1996.

[29] V. Bargmann. On a Hilbert space of analytic functions and an associated integral transform. *Commun. Pure Appl. Math.*, 14:197–214, 1961.

[30] P. Lebœuf and A. Voros. "chaos-revealing multiplicative representation of quantum eigenstates". *J. Phys. A*, 23, 1990.

[31] Perelomov, A. . *Generalized coherent states and their applications.* Springer-Verlag., 1986.

LPMMC (Maison des Magisteres Jean Perrin, CNRS) BP 166 38042 Grenoble Cedex 9 France email: faure@labs.polycnrs-gre.fr .